Electronic Applications of Polymer Electrolytes of Epoxidized Natural Rubber and Its Composites

Fatin Harun and Chin Han Chan

Abstract The hope for composite polymer electrolytes (CPE) to fulfill future electronic applications has encouraged researchers to look up for wider range of polymer candidates, which are suitable for this purpose. Epoxidized natural rubber (ENR) is one of the candidates with polar epoxy group that helps in compatibilization with other polymers and provides coordination sites for fillers and organic or inorganic salt. Besides, low glass transition temperature, good dimensional stability and impact strength, and satisfactory stickiness finally provide sufficient contact between electrolytic layer and electrode for electronic devices. The desirable properties of ENR have earned researchers' attention to further explore its potential. Hence, this work will attempt to compile and review the ENR, ENR-based, and composite ENR-based electrolytes for electronic applications, especially in ionic conductivity.

Keywords Epoxidized natural rubber · Polymer electrolytes · Ionic conductivity · Glass transition temperature · Selective localization

1 Introduction to Epoxidized Natural Rubber

1.1 Structure and Composition

Pummere and Burkard [1] were the first to report the epoxidation reaction of natural rubber (NR). Epoxidized natural rubber (ENR) is a modified form of NR in which some of the double bonds in the *cis*-polyisoprene chain have been converted to oxirane groups. The epoxy groups are randomly distributed along the backbone

F. Harun · C.H. Chan (✉)
Faculty of Applied Sciences, Universiti Teknologi MARA (UiTM),
40450 Shah Alam, Selangor, Malaysia
e-mail: cchan@salam.uitm.edu.my

D. Ponnamma et al. (eds.), *Flexible and Stretchable Electronic Composites*,
Springer Series on Polymer and Composite Materials,
DOI 10.1007/978-3-319-23663-6_2

of NR [2]. The chemistry of epoxidation of NR and the subsequent ring-opening reactions have been extensively studied by Swern [3]. Epoxidation is a stereo-specific reaction, and the rate of epoxidation is governed by the substituents on the double bond [3, 4]. Only in the mid-1980s, the pure samples of ENR were prepared and their potential applications were realized [5–7].

ENR is composed of 2-methylbut-2-ene and 2,3-epoxy-2-methylbutane units. Upon epoxidation, ENR can still undergo strain crystallization since oxygen is small enough to fit into the crystal lattice with only minor geometrical rearrangements. Therefore, it maintains the superior tensile properties of NR [8, 9]. Epoxidation is a highly exothermic reaction (60 kcal g^{-1} mol^{-1}), but under carefully controlled conditions of reaction temperatures and acid concentration below 20 w/w%, NR latex can be epoxidized to over 75 mol% without the formation of secondary ring-opened structures [7]. Nevertheless, most of the studies are limited to commercially available ENR, namely ENR-25 and ENR-50, where 25 and 50 denote 25 and 50 mol% of epoxide group. This type of chemical modification offers excellent scope of potential applications considering low cost of NR latex and simple nature of ENR production [10].

The properties of ENR change gradually with the epoxide level. Hysteresis, swelling resistance, and gas impermeability improve with increasing epoxide level, while resilience, on the other hand, decreases [5, 11]. The physical properties of ENR could be governed by increase in glass transition temperature (T_g), solubility, and ability to undergo strain crystallization [8].

The commercial production of ENR in the early time and after the year 1969 has several differences in their properties. Before 1969, the "old ENR" was known to have high Mooney viscosities of about 120, high gel contents (60–80 %) and acidic in nature (pH 6). This results in difficulty of mixing and filler dispersion in the rubber. Mixing can be optimized by premastication of the rubber in the presence of a base, but even so, filler could not be incorporated into the highly cross-linked macrogel phase causing heterogenous mixture [12].

In 1989, a different technological production of ENR known as Epoxyprene was launched by Kumpulan Guthrie Berhad, Malaysia. Epoxyprene has lower Mooney viscosities of about 80, more consistent composition, lower gel content (30–40 %), and alkaline in nature (pH 7–10), leading to easy processing of rubber. The advantages of the epoxyprene are that it can be compounded without the need of premastication, and homogenous carbon black filler distribution can be obtained [13, 14].

1.2 Synthesis Pathways

Epoxidation reaction can be carried out in solution or latex form (refer Table 1) but only latter is of commercial values. *In situ* epoxidation is preferred to minimize processing and costs [15].

Table 1 Epoxidation routes of NR

	Description
(1) Solution form	(a) Perbenzoic acid [16, 17]
	(b) Perphthalic acid [18]
	(c) Peracetic acid [19, 20]
	(d) Hydrogen peroxide/acetic mixtures catalyzed by *p*-toluene sulfonic acids [17, 19]
(2) Latex form	(a) Bromohydrin intermediates, hydrogen peroxide-catalyzed system [15] • Dibromide and bromohydrin formed during bromination, consumed bromine that was intended to react with rubber • Low efficiencies of epoxidation may be related to the difficulty in transferring water-soluble intermediate to the rubber particles
	(b) Peracetic acid [21–23] • Easy preparation using acetic anhydride and hydrogen peroxide • Low cost of reagents • Peracetic acid is stable and compatible with both aqueous and hydrocarbon phase of latex, uniform reaction • Quantitative conversion results in excellent efficiency of epoxidation • No evidence of ring-opened epoxide groups at moderately low modification level • Negligible side products when carried out under ambient temperature and in the absence of strong acid catalyst
	(c) Performic acid [15, 24, 25] • Prepared from hydrogen peroxide and formic acid • Epoxidation is accompanied by extensive amounts of secondary products • High acidity accelerates ring-opening reactions

Comparing the choices of epoxidation routes of NR, it can be concluded that epoxidation in latex using peracetic acid (refer Fig. 1) is one of the best methods of all, for laboratory scale as well as standard industrial production. To prepare latex epoxidation, it is necessary to first stabilize the latex by adding nonionic surfactant. The surface of the rubber particles surrounded by proteins is anionic charged, while peracetic acid to be added is cationic charged. Adding different charge surfactants to the NR latex would cause the rubber particles to destabilize. Therefore, nonionic surfactant must be used to stabilize NR latex against acid coagulation. After epoxidation completed, the ENR can be precipitated either by

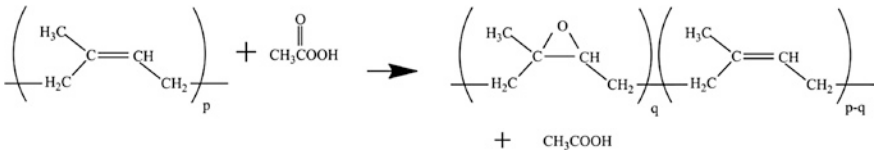

Fig. 1 Epoxidation of NR using peracetic acid

using alcohol or acetone, adding salt, or heating to temperature above the cloud point of the surfactant. Lastly, the ENR can be washed with base to remove all unreacted acid [26].

1.3 Characteristics

ENR consists of two parts namely, sol (soluble in organic solvent) and gel (insoluble in organic solvent). The sol was deduced to be intramolecular ether with linear structures, whereas gel is intermolecular ether with net-like structures [5, 27]. High cross-link structure of gel content was believed to be attributed by higher degree of epoxidation [5], minute structural changes (free radical) in ENR that may occur during milling [28], thermal effect during molding of rubber [29], interchain interactions by H-bonding through ring-opened products of ENR [29], and temperature [30]. Mild reaction conditions can avoid the ring-opening reactions. Nevertheless, the longer preparation time required is not favorable for scaled production of ENR.

1.3.1 ^{1}H-Nuclear Magnetic Resonance (^{1}H-NMR)

The determination of ENR structure using ^{1}H-NMR method (refer Table 2) was developed by Durbetaki and Miles [31]. For NR, the characteristic signals of

Table 2 Chemical shift assignment of ^{1}H-NMR for ENR

Chemical shift (ppm)	Assignment	Reference
1.7	Methyl CH_3–C=C	[32]
2.1	Methylene –CH_2–	[32]
5.1	Unsaturated methyne/olefinic hydrogen CH=C	[33]
1.3	Methyl of epoxy group CH_3–CO	[20]
2.7	Methyne of epoxy group	[20]
3.4	Diol	[2, 34]
3.9	Furan	[34]

Note ^{1}H-NMR spectrum for ENR-20

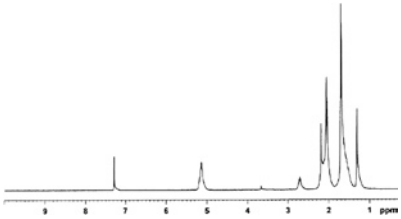

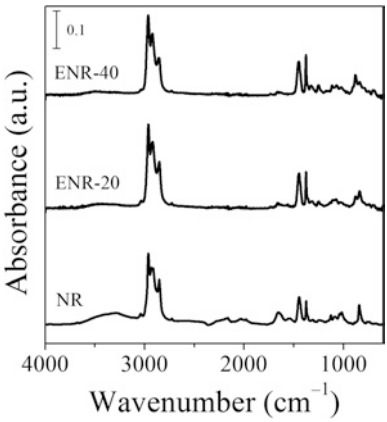

Fig. 2 FTIR spectra of NR and ENR

methyl, methylene, and unsaturated methyne protons of *cis*-1,4-isoprene units appeared at 1.7, 2.1 and 5.1 ppm, respectively. However, ENR spectrum shows two additional signals that appeared at 1.3 and 2.7 ppm which represent the methyl and methyne protons of the epoxy group, respectively.

1.3.2 Fourier Transform Infrared Spectroscopy (FTIR)

The FTIR spectra of NR and ENR are given in Fig. 2. The presence of C=C stretching (1654 cm^{-1}), CH olefin wagging (842 cm^{-1}), and CH_3 deformation (1376 cm^{-1}) confirm the identity of NR. On the other hand, ENR shows additional peak at 880 and 1250 cm^{-1} corresponding to oxirane ring and stretching vibration of C–O–C, respectively.

1.3.3 Thermal Properties

T_g of ENR increases as the amount of epoxide groups increases (refer Fig. 3). The presence of bulky epoxide group lowers the rotational freedom of the modified segment [15]. For every 1 mol% epoxidation, the T_g increases by approximately 1 °C [15, 35]. The presence of proteins in NR does not interfere with the formation of epoxide and segmental mobility of the chain [36].

The thermal stability of ENR in nitrogen atmosphere and in air exhibits different trend by thermal gravimetry analysis (TGA). In nitrogen atmosphere, ENR shows single-step decomposition. Presence of epoxy group was claimed to provide higher thermal stability in inert environment (refer Fig. 4) due to epoxide ring opening that occurs during the test which consequently slows down the rubber degradation [37]. On the other hand, presence of epoxy group destabilizes thermal

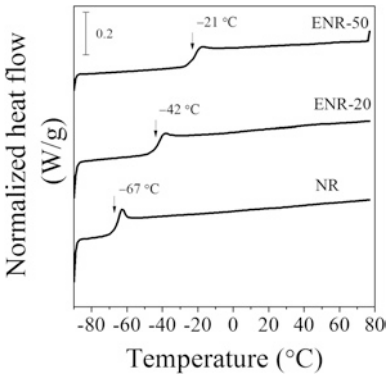

Fig. 3 DSC traces of reheating cycle for NR and ENRs

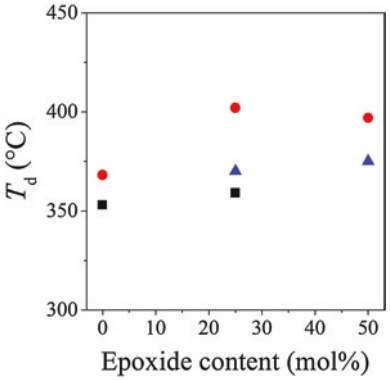

Fig. 4 Onset of thermal degradation temperature of ENR in nitrogen atmosphere, *square* [39], *circle* [40], and *triangle* [unpublished result]

stability of ENR in air. Thermal degradation of ENR in air shows two-step decomposition [27, 38]. The steps are in the range of 200–450 °C (approaches first-order reaction) and 450–550 °C, respectively.

1.3.4 X-ray Diffraction

NR can undergo strain-induced crystallization where the unit cell was reported to be orthorhombic (92°) or monoclinic (90°) [41, 42]. Meanwhile, ENR also displays the same unit cell where the volume increases with degree of epoxidation (refer Table 3). Beyond 50 mol%, the degree of crystallinity reduces drastically which may imply that the basic unit of NR can accommodate two epoxide groups [7, 8].

Table 3 Unit cell volume and degree of crystallinity estimated by X-ray diffractometer for ENR vulcanizates (2 phr sulfur) at 400 % strain. Copyright 1987 reprinted with permission from [13]

ENR	Unit cell volume (nm^3)	Degree of crystallinity
NR	0.955	11
ENR-25	0.985	11
ENR-50	0.999	10
ENR-75	1.036	4
ENR-90	1.036	2

Table 4 Mechanical properties of NR, ENR-25, and ENR-50

	NR	ENR-25	ENR-50
Modulus at 100 % elongation (MPa)	0.25 [39]	0.20 [39]	0.33 [44]
Elongation at break (%)		322 [14]	482 [14] 267 [44]
Green strength (MPa)[a]		0.34 [14]	0.49 [14]
Wallace plasticity	45 [14]	33 [14]	40 [14]
Plasticity retention index	>50 [14] 66 [45] 3 (after solvent extraction) [14]	45 [14]	45 [14] 22 [45]
Tensile strength (kPa)			548 [44]
Shore A hardness			15 [44]

[a]Green strength can be defined as resistance to deformation and fracture before vulcanization

1.3.5 Mechanical Properties

ENR becomes mechanically harder with increasing epoxide contents. This is related to the increased T_g of this modified NR [15]. Despite that, below 25 mol% modification, ENR is as elastic as NR [43]. Resilience of ENR decreases with increasing amount of epoxide, improving its wet grip performance. Some mechanical properties of ENR are summarized in Table 4.

1.3.6 Air Permeability

The air permeability of ENR is dependent on the level of epoxidation (refer Table 5). Epoxidation lowers the air permeability due to reduced segmental rotation rates and higher ENR density [11, 15].

Table 5 Air permeability of ENR. Copyright reprinted with permission from [46]

	Air permeability ($m^4\ s^{-1}\ N^{-1} \times 10^{18}$)
NR	28.1
ENR-10	14.8
ENR-25	5.9
ENR-50	1.9

1.3.7 Aging Behavior

Wong and Ong [14] studied the aging behavior of NR, ENR-25, and ENR-50 at 50, 70, and 90 °C, respectively. As temperature increases, reduction in Wallace plasticity can be observed in ENR where the effect is more significant in higher epoxide rubber and at higher temperature (refer Fig. 5). Green strength, elongation, and modulus of stress–strain properties of ENR show no significant increase upon aging (refer Table 6). The amount of gel and epoxide content in ENR was found to remain consistent even when they were aged at 70 °C.

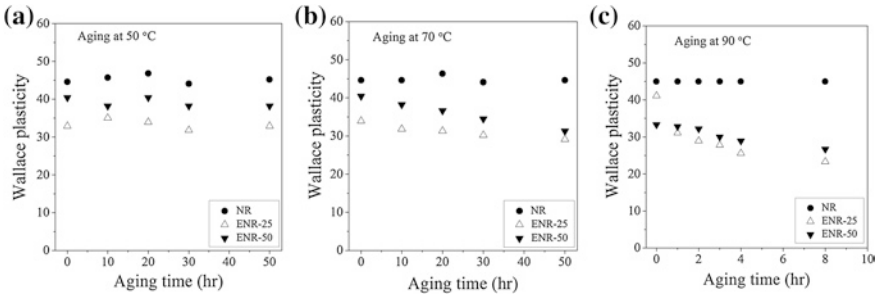

Fig. 5 Changes in Wallace plasticity at different temperatures, **a** 50 °C, **b** 70 °C, **c** 90°C. Copyright reprinted with permission from [14]

Table 6 Green strength and elongation at break of aging ENR. Copyright reprinted with permission from [14]

	ENR-25				ENR-50			
	Unaged	Aged at 50 °C			Unaged	Aged at 50 °C		
		4 h	16 h	32 h		4 h	16 h	32 h
Green strength (MPa)	0.34	0.21	0.26	0.24	0.49	0.42	0.40	0.37
Elongation at break (%)	322	327	307	310	482	513	493	447

1.4 Techniques to Determine Epoxide Content

There are many techniques to determine epoxide content of ENR. The most convenient and reliable method would be using ^{1}H-NMR and DSC. The advantages and disadvantages of each technique are summarized (refer Table 7).

Table 7 Various methods in determining epoxide content of ENR

Method	Techniques to determine epoxide content
1. ^{1}H-NMR [47]	Ratio of integrated areas of the olefinic and epoxy methane protons $\text{Mol\% epoxide} = \left(\frac{A_{2.70}}{A_{5.14}+A_{2.70}}\right)$ In the range of 25–70 mol%, reproducibility was found to be ±1.5 %
2. ^{13}C-NMR [20]	$\text{Mol\% epoxide} = \frac{100(A_{64.5})}{A_{64.5}+A_{124.4,125.0,125.7}}$ In the range of 25–70 mol%, reproducibility was found to be ±0.8 %
3. Elemental analysis	%C, %H and %O Large divergent of reproducibility: 12.9 % Possibility of sample inhomogeneity which would be accentuated by small samples required for microanalysis
4. HBr titration [48]	Direct titration of oxirane ring with HBr is essentially quantitative and with few interferences for ENR at low modification level (<5 mol%) Rapid technique being appropriate <15 mol% where spectroscopic techniques are less accurate Limited solubility at higher modification level as well as cyclization side reactions between adjacent oxirane rings
5. Differential scanning calorimetry (DSC) [49]	T_g of ENR increases linearly with epoxy content $\text{Mol\% epoxide} = \frac{T_g+70}{0.92}$ Reproducibility: 0.25 % Presence of significant side products derived from cyclization, hydrolysis, or esterification would nullify validity of calibration
6. Density [15]	T_g value is directly related to polymer density (density vs. T_g plot) Epoxide content (%) / T_g (°C) / Density (g/cm^3) 0 / −66.4 / 0.898 10 / −60.3 / 0.906 20 / −53.0 / 0.917 35 / −42.2 / 0.937 50 / −30.1 / 0.965 65 / −16.6 / 0.986 Convenient low-cost measure of epoxy content The progressive increase in T_g parallels with increase in polymer density due to reduction in volume of the chain segments

(continued)

Table 7 (continued)

Method	Techniques to determine epoxide content
7. FTIR [50, 51]	(a) Lambert–Beer law to calculate percentage of epoxy groups of ENR $C_e = \frac{100k_1A_2}{A_1+k_1A_2+k_2A_3}$ $C_d = \frac{C_2A_1}{k_1A_2}$ $C_o = 100 - C_d - C_d$ $A_1 = A_{835}$ $A_2 = A_{870}–0.14A_{835}$ $A_3 = A_{3460}–0.019A_{1375}$ where C_e, C_d, and C_o are the molar percentage of epoxy groups, carbon–carbon double bonds, and ring-opening products, respectively. A_{835}, A_{870}, A_{1375}, and A_{3460} are the absorbencies corresponding to 835, 870, 1375, and 3460 cm^{-1}. The values of k_1 and k_2, calculated from the C_e and C_d values determined from NMR method, are 0.77 and 0.34, respectively (b) Mol% epoxide $= \left(\frac{A_{874}}{A_{840}+A_{874}}\right)$

1.5 Applications of ENR

ENR has been utilized in various fields since the past such as automotives [52], substitute of acrylonitrile butadiene and butyl rubber products [50], coating [39, 53], clamping [54], wire and cabling [55], adhesions and sealants [56, 57], compatibilizer [58], and toughening agent in plastics [59, 60]. Recently, ENR is being featured as autonomous healing materials [61, 62] and for electronic applications [63–70] something uncommon and outside the traditional uses of rubber. In the next section, we will focus on the electronic applications of composite ENR-based polymer electrolytes, and in particular, we concentrate on impedance results.

2 Electronic Applications of ENR

2.1 Solid Polymer Electrolytes (SPEs)

SPE is made up of metal salt that dissolves in the polar matrix polymer to form a solid salt solution [71]. It has favorable mechanical strength, ease in fabrication of thin films into desirable size, and its ability to form effective electrode–electrolyte contacts [72]. Over many years, SPEs still remain the potential of interest for various applications in electrochemical devices, such as separators or electrolyte membranes in high energy density lithium-ion rechargeable batteries, fuel cell membrane, electrochromic displays, photoelectrochemical devices, smart windows, data storage, sensors, transistors, supercapacitors, and many more [71, 73, 74]. Therefore, it is desirable for SPEs to show acceptable conductivities

(~10^{-3} to 10^{-4} S cm^{-1}) at room temperature, dimensional stability, and elastomeric properties [73, 75].

The common polymer hosts used are thermoplastics such as poly(ethylene oxide) (PEO) [76–78], polyacrylonitrile (PAN) [79], poly(vinyl alcohol) (PVA) [80, 81], and poly(vinylidene fluoride) (PVDF) [82, 83]. Despite that, their conductivity is not high enough at room temperature. While ionic transport takes place mainly in amorphous phase, high degree of crystallinity in the semicrystalline polymer hosts (e.g., PEO) at room temperature is not favorable.

In view of that, ENR could be a potential candidate for SPE system. It has polar epoxy oxygen, low T_g, and amorphous nature that are suitable for ionic percolation at room temperature. In addition, ENR also offers flexibility and good contact between electrolytic layer and electrode for electronic devices [70].

2.1.1 ENR

Idris et al. [70] were the first to study ENR-based SPEs. They suggest that complexation between lithium cation (Li^+) and epoxy oxygen of ENR is similar to the mechanism of PEO and Li^+, the oldest and widely studied SPE system. The formation of transient cross-links of intra- and intermolecular coordination of oxygen atom in ENR with Li^+ restricts the segmental motion of ENR chains which in turn increase the T_g values. Above certain salt concentration, T_g value fluctuates when the level of transient cross-link is high enough to reduce Li^+ and polymer chain mobility, and distribution of salt becomes inhomogeneous. Under this condition, the salt–salt interactions are preferred than salt–polymer interactions [84].

As mentioned in previous section, properties of ENR changes gradually with epoxidation degree. Nevertheless, this effect was seldom considered and discussed. Yusoff et al. [85] have well demonstrated that ENR with more epoxy group will have stronger interaction with salt due to more coordination sites for Li^+ transport (see Fig. 6). The similar T_g trend is observed by Klinklai et al. [86] as

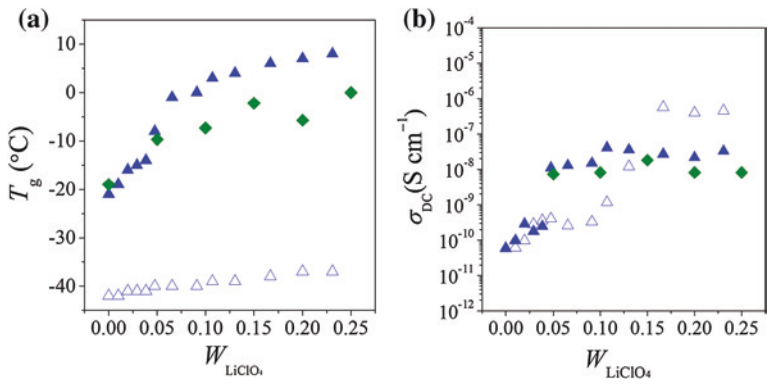

Fig. 6 **a** Glass transition temperature and **b** ionic conductivity of ENR/$LiClO_4$. *Open triangle* [85] indicates ENR-25; *filled triangle* [85] and *filled diamond* [67] indicate ENR-50

Table 8 Ionic mobility and diffusion coefficient of ENR/$LiClO_4$ ranging from $W_s = 0$–0.13 estimated from impedance spectrometer. Copyright reprinted with permission from [85]

	ENR-25	ENR-50
Ion mobility, $\alpha\mu$ ($cm^2\ V^{-1}\ s^{-1}$)	3.3×10^{-11}	4.4×10^{-10}
Diffusion coefficient, D ($cm^2\ s^{-1}$)	8.5×10^{-13}	1.1×10^{-11}

well. From FTIR study, a stronger ion–dipole interaction at C–O–C of ENR-50 with $LiClO_4$ was observed as compared to ENR-25. It is noted that Li^+ ions prefer to coordinate with epoxy oxygen than with the C=C bonds. ENR-50 has higher conductivity than ENR-25 when the weight percent of salt (W_s) < 0.15, which could be due to higher ion mobility, better salt molecular-chain segment correlation, and higher charge carrier diffusion rate (refer Table 8). When $W_s > 0.15$, the conductivity of ENR-50 is lower than ENR-25. This is because at high salt concentration, conductivity of ENR is dominantly governed by segmental motion rather than charge carrier density. The study suggests that polarization relaxations cause formation of stable percolation network, leading to significant increase in conductivity at $W_s = 0.05$–0.11 for ENR-50 and $W_s = 0.11$–0.17 for ENR-25. The results disagree with initial findings by Idris et al. [70] that report that ENR-25 has higher conductivity than ENR-50 at relatively high salt content.

The dielectric study done by Chan et al. [87] on ENR-25 doped with $LiClO_4$ indicates a non-Debye relaxation. The stable resistor networks only occur at $W_s \geq 0.2$. Molar conductivity indicates Kohlrausch-like variation over a certain range of concentration. The nonlinear deviation of molar conductivity at low salt concentration and unaffected polarizability of ENR-25 signifies the weak interaction between ENR-25 chains and salt molecules. For ENR-50 doped $LiClO_4$, Chan and Kammer [88] revealed that the values of diffusion coefficient and degree of dissociation (10^{-5}) remain constant over a wide range of $LiClO_4$ concentration ($W_s \leq 0.17$).

Tan et al. [67] studied the influence of various anions of lithium salts in ENR-50. The order of interaction strength between ENR and Li salt is $LiBF_4$ < $LiClO_4$ < LiI < $LiCF_3SO_3$ < $LiCOOCF_3$. However, the conductivity does not correlate well with the interaction strength: $LiBF_4 > LiCF_3SO_3 \sim LiCOOCF_3 > LiI > LiClO_4$. In this work, lattice energy explains the conductivity behavior where lower lattice energy salt dissociates easily and thus has more charge carrier and higher conductivity. Despite that, $LiClO_4$ could not be explained using the same factor because $LiClO_4$ was said to have high ion pair formation which causes number of charge carrier to decrease and finally low conductivity performance. In terms of thermal stabilization, it was found out that $LiClO_4$ destabilizes while $LiBF_4$ enhances the thermal stability of ENR (due to cross-link reaction). The rest of the salts studied do not significantly affect the decomposition temperature of ENR, in agreement with FTIR and DSC results.

Table 9 summarized previously reported conductivity studies on ENR-based SPE. The values are too low for application. It is interesting to note that the strong interaction strength between salt and ENR does not necessarily ensure a

Table 9 Previously reported conductivity on various ENR-based SPE at room temperature

System	σ_{max} (S cm^{-1})	Reference
ENR-50/LiN(SO_2CF_3)$_2$	4.6×10^{-5}	[91]
ENR-50/$LiBF_4$	2.7×10^{-5}	[67]
ENR-25/$LiCF_3SO_3$	6.2×10^{-5}	[70]
ENR-50/$LiCF_3SO_3$	2.3×10^{-5}	[70]
	9.3×10^{-7}	[67]
ENR-50/$LiCOOCF_3$	2.0×10^{-6}	[67]
ENR-50/LiI	2.7×10^{-7}	[67]
ENR-25/$LiClO_4$	5.7×10^{-7}	[85]
ENR-50/$LiClO_4$	4.1×10^{-8}	[85]
	1.8×10^{-8}	[67]

high conductivity. There are many other factors to be considered such as ion salvation (lattice energy of salt), deformation of polymer structure due to inclusion of salt, and segmental movement of the polymer chains [89, 90]. Moreover, same ENR-based SPE system may not have similar ionic conductivity, for example, ENR-50/$LiCF_3SO_3$, as shown in Table 9. Those two separate studies on the same system show one order of conductivity difference. This could be due to difference in molecular weight of ENR, effect of non-rubber component (gel, protein), sample preparation, etc. Therefore, variation from ENR itself should be minimized to have fair comparison.

2.1.2 ENR Composites

Composite polymer electrolytes (CPE) introduced a filler which is dispersed to SPE as a third component. Inorganic fillers have been used since the 1980s where micrometer-sized ceramic particles were added to improve the mechanical properties. Later, nano-sized particles such as Al_2O_3, SiO_2, TiO_2, and ZrO_2 were used in attempt to enhance the conductivity as well. Although many studies were conducted about CPE, the conductivity behavior is still not well understood until now. Using effective medium theory (EMT) models, Wieczorek and Siekierski [92] explained that the dispersed filler particles are assumed to be surrounded by interface regions with an enhanced conductivity over the bulk electrolyte. However, this theory does not explain the reasons of conductivity differences in the interfacial regions. Several authors pointed out the relationship of Lewis acid–base interactions in describing the conductivity increase. Wieczorek et al. demonstrated the validity of the Lewis acid–base approach for various semicrystalline and amorphous systems [93, 94]. In 2001, Best et al. [95] described the conductivity behavior using a simple electrostatic model where he explained that the lithium cations experience the same potential at TiO_2 filler surfaces as at the polymer. This means that the lithium ions can move between these sites with a lower activation energy

barrier. Later, they propose that the conductivity increase is due to the formation of percolating interface regions which allows the formation of conduction pathway interface near filler particles [96].

Tan and Bakar [97] studied thermal properties of ENR-50/$LiCF_3SO_3$ added with nano-sized Fe_3O_4. Trend of T_g follows as: ENR < ENR/Fe_3O_4 < ENR/$LiCF_3SO_3$/Fe_3O_4 < ENR/$LiCF_3SO_3$. Fe_3O_4 has negligible interaction with ENR in composite. However, in CPE, competing interactions occur between salt and filler or with ENR chains. In nitrogen atmosphere degradation, the trend of activation energy is: ENR/Fe_3O_4 < ENR/$LiCF_3SO_3$/Fe_3O_4 < ENR < ENR/$LiCF_3SO_3$. In CPE, salt suppresses catalytic effect of filler on the degradation of ENR. No conductivity study of the system was reported here.

2.1.3 ENR-Based Blends

Polymer blends are a mixture of two or more different polymers together. It can be classified into two main categories which are miscible and immiscible blends. Blending ENR with another polymer host, SPE may enhance the conductivity and mechanical properties.

An example of immiscible ENR-based SPE blends is PEO/ENR/$LiClO_4$. Chan and Kammer [98] found two T_g(s) with respect to PEO and ENR-50 over the entire composition range where both increase with addition of salt. Findings from T_g values show almost equal salt solubility in both polymers, but slower rates of crystallization and conductivity enhancement suggest that salt has higher solubility in PEO of the blend. The same PEO/ENR blends were studied by Noor et al. [99, 100], using $LiCF_3SO_3$ salt. The systems obey Arrhenius rule for temperature dependence impedance study. The salt-added PEO/ENR 70/30 blend has lower activation energy and higher conductivity pre-exponential factor as compared to PEO/$LiClO_4$. This indicates that the energy required to dissociate cations from anions and the mobility of charge carrier in the blend electrolyte is smaller. $LiCF_3SO_3$ decreases the thermal stability of PEO/ENR. Studies of Noor et al. [99, 100] and Chan et al. [87, 98] point toward preferential localization of lithium salt in PEO phase of the immiscible blends of PEO/ENR (when PEO is the major component) after T_g analysis using DSC, ion–dipole interaction using FTIR, etc. This leads to concentration of salt in PEO that becomes more concentrated in blends as compared to the neat PEO. Hence, the conductivity of salt-containing blends shall be higher than that of salt-containing PEO with addition of equivalent amount of salt.

It is important to stress that incorporation of ENR as minor component in other immiscible blends such as PVDF/ENR-50/$LiCF_3SO_3$ and PMMA/ENR-50/$LiCF_3SO_3$ also leads to very similar results where the polymer blend electrolytes exhibit higher conductivity as compared to PVDF/$LiCF_3SO_3$ and PMMA/$LiCF_3SO_3$, respectively. PVDF/ENR-50/$LiCF_3SO_3$ blend ratio of 60/40 at $W_s = 0.20$ shows highest conductivity (4.0×10^{-5} S cm^{-1}) for the system. The appreciable increase in T_g of PVDF demonstrates that lithium salt tends to interact more with PVDF than ENR [101]. For PMMA/ENR-50/$LiCF_3SO_3$

system, blend composition of 90/10 at $W_s = 0.60$ exhibits highest conductivity (5.1×10^{-5} S cm^{-1}). The ion–dipole interaction in FTIR characterization hints toward selective localization of lithium salt in PMMA [102].

PVC/ENR/$LiClO_4$ system also reveals higher conductivity than PVC-doped $LiClO_4$. Despite that, highest conductivity enhancement was obtained when ENR was employed as the major phase, which is different than the examples mentioned above. At constant salt content ($W_s = 0.40$), PVC/ENR 30/70 blend shows higher conductivity (6.8×10^{-8} S cm^{-1}) as compared to 70/30 (8.6×10^{-9} S cm^{-1}). Parameters other than impedance study were not discussed much in the literature; hence, localization of salt in these blends could not be concluded [103].

Besides achieving higher conductivity, polymer blends were also employed to provide mechanical strength. Mohammad et al. [104] studied ENR-50/polyethyl methacrylate (PEMA)/$NH_4CF_3SO_3$. The purpose of adding PEMA as a second component is to give mechanical strength where 60/40 blend ratio produces free standing film. Highest conductivity for this blend ratio (5.4×10^{-6} S cm^{-1}) is obtained when $W_s = 0.40$. This value is lower than PEMA/$NH_4CF_3SO_3$ (1.0×10^{-5} S cm^{-1}) [104, 105]. Only one T_g value (~5 °C) was observed in which the value is nearer to the T_g of ENR-50 (−21 °C) as compared to PEMA (65 °C). A more detailed study should be carried out to determine the miscibility of the blends.

Many assumptions and suggestions have been made in attempt to explain the conductivity enhancement in ENR-blend SPE. Most polymer blends are immiscible from the thermodynamic standpoint. The effect of phase separation of SPE binary blends due to preferential localization of salt in different phases is not so well explained except in Refs. [87, 98, 106]. Table 10 summarized the reported

Table 10 Previously reported conductivity on various ENR-blend SPE at room temperature

System	Composition	σ_{max} (S cm^{-1})	Reference
PEO/$LiClO_4$ PEO/ENR-50/$LiClO_4$ $T_{g,\,PEO} = -54$ °C $T_{g,\,ENR\text{-}50} = -19$ °C	$W_s = 0.15$ 60/40; $W_s = 0.11$	7.9×10^{-6} 8.0×10^{-5}	[107] [93]
PEO/$LiCF_3SO_3$ PEO/ENR-50/$LiCF_3SO_3$	$W_s = 0.15$ 70/30; $W_s = 0.20$	2.1×10^{-6} 1.4×10^{-4}	[99]
PVdF/$LiCF_3SO_3$ PVdF/ENR-50/$LiCF_3SO_3$ $T_{g,\,PVdF} = -40$ °C [108]	Not mentioned 60/40; $W_s = 0.20$	1.4×10^{-5} 2.7×10^{-5}	[101]
PMMA/$LiCF_3SO_3$ PMMA/ENR-50/$LiCF_3SO_3$ $T_{g,\,PMMA} = 120$ °C	$W_s = 0.40$ 90/10; $W_s = 0.60$	4.9×10^{-8} 5.1×10^{-5}	[102]
PEMA/$NH_4CF_3SO_3$ PEMA/ENR-50/$NH_4CF_3SO_3$ $T_{g,\,PEMA} = 65$ °C	$W_s = 0.35$ 40/60; $W_s = 0.40$	1.0×10^{-5} 5.4×10^{-6}	[105] [104]
PVC/$LiClO_4$ PVC/ENR/$LiClO_4$ $T_{g,\,PVC} = 82$ °C [109]	$W_s = 0.20$ 30/70; $W_s = 0.30$	8.8×10^{-10} 8.5×10^{-7}	[109] [103]

Table 11 Ionic conductivity of PEO/ENR-50/$LiCF_3SO_3$ in 70/30 blend at $W_s = 0.30$. Copyright reprinted permission from [110]

Weight percent of ZnO (%)	Ionic conductivity (S cm^{-1})
0	1.39×10^{-4}
2	1.02×10^{-5}
4	1.25×10^{-5}
6	4.60×10^{-6}
8	2.54×10^{-6}

conductivity for ENR-blend SPE. Interestingly, when ENR is blended with another polymer host, sometimes ENR must be retained as minor phase (blends with PEO, PVdF, PMMA) and sometimes as major phase (blends with PVC) to achieve higher conductivity. In general, the use of ENR as dispersed phase to lead salt to become more concentrated in the major phase that governed the ionic conductivity in the immiscible blends allows lower percolation threshold that contributes to the enhancement of conductivity. Nevertheless, the preferential localization of salt is yet to be fully resolved. Detailed T_g study using Nernst distribution coefficient [87, 98, 106] could provide some insight on the distribution of salt among the blend constituents.

2.1.4 ENR-Blend Composites

Noor et al. [110] investigated the PEO/ENR-50/$LiCF_3SO_3$/nano-ZnO system. Surface morphology showed that ZnO was uniformly dispersed at low concentration, but the filler made the surface rough. Addition of ZnO causes reduction of ionic conductivity by one to two order of magnitude (refer Table 11). They suggest that filler causes blocking effect on ion transport, reduce effective interaction between polymer blends and salt, and unsuccessful in increasing number of ion dissociation. This explanation calls for future investigation.

2.2 Gel Polymer Electrolytes (GPEs)

GPE is a liquid electrolyte immobilized in polymer matrix. Normally, it has ionic conductivity about 10^{-3} S cm^{-1} at room temperature. However, GPE has its own drawback where it lacks mechanical stability to produce thin films. The liquid electrolyte can permeate into the polymer which ends up softening the polymer [111, 112].

2.2.1 ENR

Idris et al. [70] found that plasticized ENR-25/$LiCF_3SO_3$ electrolytes show higher conductivity than plasticized ENR-50/$LiCF_3SO_3$. Incorporation of plasticizer causes tremendous increase in conductivity and reduction in T_g. Mohamed et al.

Table 12 Ionic conductivity of ENR-based GPE at room temperature

System	Composition (w/w/w)	σ (S cm^{-1})	Reference
ENR-50/$LiCF_3SO_3$/EC	100/35/20	2.4×10^{-4}	[113]
ENR-50/$LiCF_3SO_3$/PC	100/35/10	4.9×10^{-4}	
ENR-25/$LiCF_3SO_3$/EC + PC	100/5/100	1.4×10^{-4}	[70]
ENR-25/$LiCF_3SO_3$/EC + PC	100/5/200	2.9×10^{-4}	
ENR-50/$LiCF_3SO_3$/EC + PC	100/5/100	4.0×10^{-5}	[70]
ENR-50/$LiCF_3SO_3$/EC + PC	100/5/200	1.3×10^{-4}	
ENR-50/$LiN(SO_2CF_3)_2$/EC + PC	100/5/50	5.8×10^{-4}	[91]
	100/5/100	8.4×10^{-4}	
	100/5/150	2.6×10^{-3}	

[113] studied ENR-50/$LiCF_3SO_3$ plasticized with EC and PC. The system obeys Vogel–Tamman–Fulcher rule, which describes conductivity based on the free-volume model. The presence of plasticizer causes the entropy configuration of ENR-50 to favor the provision of more free volume where ions can move easily through plasticizer-rich phase. The dielectric study shows that presence of salt and plasticizer at certain concentrations causes an increase in dielectric constant at lower frequencies that support that high conductivity is achieved for samples that have highest concentration of free ions. PC plasticized system has higher conductivity and better electrochemical performance than EC. Table 12 summarized reported studies for ENR-based GPE.

2.2.2 ENR Blend

Latif et al. [114] studied PMMA/ENR-50/$LiCF_3SO_3$/EC. The conductivity increases after addition of 20 % EC but decreases when plasticizer amount reached 40 % and above. Only morphology and impedance study were reported here. Therefore, detailed characterizations are required to compare the plasticized and unplasticized system.

Rahman et al. [115] studied PVC/liquid ENR-50 (LENR)/$LiClO_4$/PC. The conductivity increases with addition of plasticizer and reaches maximum when 70 % of PC was added. Not much information could be drawn out from the conductivity, morphology, and FTIR studies reported. The ionic conductivity of ENR blend-based GPE is summarized in Table 13.

Table 13 Ionic conductivity of ENR blend-based GPE at room temperature

System	Composition	σ (S cm^{-1})	Reference
PVC/LENR-50/$LiClO_4$	$W_s = 0.30$	2.3×10^{-8}	[116]
PVC/LENR-50/$LiClO_4$/EC	30/70/70; $W_s = 0.30$	2.1×10^{-7}	[115]
PMMA/ENR-50/$LiCF_3SO_3$	90/10;	5.1×10^{-5}	[102]
PMMA/ENR-50/$LiCF_3SO_3$/EC	$W_s = 0.60$ Not mentioned	4.1×10^{-7}	[114]

3 Conclusion

The research for electronic applications in ENR-based systems is still scant. The improvement of ionic conductivity through utilization of ENR as a second component has become one of the promising ways to overcome the mechanical strength and low conductivity problem at room temperature. Until then, many challenges must be addressed to fully explore its potential. It has been noted that composition of ENR itself may introduce many variations of properties as compared to NR.

The effort to achieve acceptable conductivity while maintaining sufficient dimensional stability is not an easy task. The fundamental understanding of localization of salt in the different phase of immiscible binary polymer blend host and conductivity mechanism would provide a great advantage in controlling the properties. Phase separation of the multicomponent in the blends can be used as an effective tool to control the preferential localization of salt or filler in different phases, which maintain the percolation pathways. In general, the salt percolation threshold can be decreased by preferential localization of salt in the multiphase polymer materials.

With limiting studies in ENR-based CPEs, it could not be concluded at the moment on the criteria of the filler needed for the improvement of the conductivity properties of ENR or ENR blends. The problem that calls for attention is to choose inert or functionalized filler, where the functionalized filler may enhance the interaction of salt with polymer or cause repulsion of salt and polymer to be used as a polymer electrolyte. Interactions of filler with polymer, filler with salt, and salt with polymer; morphology; T_g(s) of polymer(s); location of salt; and filler in the multiphase system have led to huge challenge in generalization of selection criteria for filler.

References

1. Pummere R, Burkard PA (1922) Uber Kautschuk. Ber Dtsch Chem Ges 55:3458–3472
2. Davey JE, Loadman MJR (1984) A chemical demonstration of the randomness of epoxidation of natural rubber. Br Polym J 16:134–138
3. Swern D (1947) Electronic interpretation of the reactions of olefins with organic peracids. J Am Chem Soc 69:1692–1698
4. Rosowsky A (1964) Ethylene oxides. In: Weissberger A (ed) Chemistry of heterocyclic compounds. Wiley, Hoboken
5. Baker CSL, Gelling IR, Newell R (1985) Epoxidized natural rubber. Rubber Chem Technol 58:67–85
6. Gelling IR, Morrison NJ (1985) Sulphur vulcanization and oxidative ageing of epoxidized natural rubber. Rubber Chem Technol 58:243–257
7. Gelling IR (1988) Chemistry, structure and properties of epoxidised natural rubber. In: Proceedings international rubber technology conference, Penang, Malaysia, 17–19 October 1988, pp 415–427
8. Davies CKL, Wolfe SV, Gelling IR, Thomas AG (1983) Strain crystallization random copolymers produced by epoxidation of *cis*-1,4-polyisoprene. Polymer 24:107–113

9. Gelling IR, Porter M (1988). Natural rubber science and technology. In: Roberts AD (ed), Oxford University Press, Oxford, p 359
10. Cizravi JC, Naginlal C, Lim SL (1999) Moisture-sorption properties and studies on the dilute solution behavior of epoxidized rubber. J Appl Polym Sci 73:1633–1644
11. Roux C, Pautrat R, Cheritat R, Ledran F, Danjard JC (1967) Modification de Polymères Insaturés par Époxydation. J Polym Sci Part C Polym Symp 16:4687–4693
12. Abu A, Sidek D (1989) Easy processing epoxidised natural rubber. J Nat Rubber Res 4:119–132
13. Gelling IR (1987) Epoxidized natural rubber. Nat Rubber Technol 18:21–29
14. Wong ST, Ong LM (1992) Storage stability of epoxyprene. Kautsch Gummi Kunstst 45:284–286
15. Burfield DR, Lim KL, Law KS (1984) Epoxidation of natural rubber lattices. J Appl Polym Sci 29:1661–1673
16. Saffer A, Johnson BL (1948) Measurement of internal double bonds in polymers by perbenzoic acid addition. Rubber Chem Technol 21:821–829
17. Kolthoff IM, Lee TS, Mairs MA (1973) Use of perbenzoic acid in analysis of unsaturated compounds. J Appl Polym Sci Poly Chem Ed 2:206–220
18. Roux C, Pautrat R, Cheritat R, Pinazzi C (1964) Epoxidation of 1,4-*cis*-polyisoprenes. Comptes Rendus 258:5442–5445
19. Mairs JA, Todd J (1932) The oxidation of caoutchouc, Gutta-percha and Balata with hydrogen peroxide. J Chem Soc 29:386–399
20. Gemmer RV, Golub MA (1978) ^{13}C NMR spectroscopic study of epoxidized 1,4-polyisoprene and 1,4-polybutadiene. J Polym Sci Polym Chem Ed 16:2985–2990
21. Gelling IR, Smith JF (1979) Controlled viscosity by natural rubber modification. In: Proceedings of the international rubber conference, Venice, Italy, 3–6 October 1979, pp 140–149
22. Saito T, Klinklai W, Yamamoto Y, Kawahara S, Isono Y, Ohtake Y (2010) Quantitative analysis for reaction between epoxidized natural rubber and poly(L-lactide) through ^{1}H-NMR spectroscopy. J Appl Polym Sci 115:3598–3604
23. Abd El Rahman AMM, El-Shafie M, El Kholy SA (2012) Modification of local asphalt with epoxy resin to be used in pavement. Egypt J Petrol 21:139–147
24. Ng SC, Gan LH (1981) Reaction of natural rubber latex with performic acid. Eur Polym J 17:1073–1077
25. Xu K, He C, Wang Y, Luo Y, Liao S, Peng Z (2012) Preparation and characterization of epoxidized natural rubber. Adv Mater Res 396:478–481
26. Bradbury JH, Perera MCS (1988) Advances in the epoxidation of unsaturated polymers. Ind Eng Chem Res 27:2196–2203
27. Yu H, Zeng Z, Lu G, Wang Q (2008) Processing characteristics and thermal stabilities of gel and sol of epoxidized natural rubber. Eur Polym J 44:453–464
28. Gelling IR (1985) Modification of natural rubber latex with peracetic acid. Rubber Chem Technol 58:86–96
29. Kumar NR, Roy S, Gupta BR, Bhomic AK (1992) Structural changes in rubber during milling. J Appl Polym Sci 45:937–945
30. Ivan G, Giurginca M, Jipa S, Tavaru E, Setnescu T, Setnescu R (1993) Thermo-oxidative behavior of epoxidised natural rubber. J Nat Rubber Res 8:31–36
31. Durbateki AJ, Miles CM (1965) Near infrared and nuclear magnetic resonance spectrometry in analysis of butadiene polymers. Anal Chem 37:1231–1235
32. Hallensleben ML, Schmidt HR, Schuster RH (1995) Epoxidation of poly(*cis*-1,4-isoprene) microgels. Die AngewandteMakromolekulareChemie 227:87–99
33. Duch MW, Grant DM (1970) Carbon-13 chemical shift studies of the 1,4-polybutadienes and the 1,4-polyisoprenes. Macromolecules 3:165–174

34. Jayawardena S, Reyx D, Durand D, Pinazzi CP (1983) Synthesis of macromolecular antioxidants by reaction of aromatic amines with epoxidized polyisoprenes, 1. Model reactions of aniline with 3,4-epoxy-4-methylheptane and with 1,2-epoxy-3-ethyl-2-methylpentane. Die Makromolekulare Chemie Rapid Communications 4:449–453
35. Saendee P, Tangboriboonrat P (2006) Latex interpenetrating polymer networks of epoxidised natural rubber/poly(methyl methacrylate): an insight into the mechanism of epoxidation. Colloid Polym Sci 284:634–643
36. Eng AH, Tanaka Y, Gan SN (1997) Some properties of epoxidized deproteinized natural rubber. J Nat Rubber Res 12:82–89
37. Heping Y, Sidong L, Zheng P (1999) Preparation and study of epoxidized natural rubber. J Therm Anal Calorim 58:293–299
38. Roy S, Gupta BR, Chak TK (1993) Studies on the ageing behaviour of gum epoxidized natural rubber. Kautsch Gummi Kunstst 46:293–296
39. Jorge RM, Lopes L, Benzi MR, Ferreira MT, Gomes AS, Nunes RCR (2010) Thiol addition to epoxidized natural rubber: effect of the tensile and thermal properties. Int J Polym Mater 59:330–341
40. Tanrattanakul V, Wattanathai B, Tiangjunya A, Muhamud P (2003) In situ epoxidized natural rubber: improved oil resistance of natural rubber. J Appl Polym Sci 90:261–269
41. Morss HA (1938) An X-ray study of stretched rubber. J Am Chem Soc 60:237–241
42. Bunn CW (1942) Molecular structure and rubber-like elasticity I: the crystal structure of *β* Gutta-Percha, rubber and polychloroprene. Proc R Soc Lond Ser A 180:40
43. Bac NV, Huu CC (1996) Synthesis and applications of epoxidized natural rubber. J Macromol Sci Pure Appl Sci A33:1949–1955
44. Ratnam CT, Nasir M, Baharin A, Zaman K (2000) Electron beam irradiation of epoxidized natural rubber. Nucl Instrum Methods Phys Res B 171:455–464
45. Perera MCS (1990) Reaction of aromatic amines with epoxidized natural rubber latex. J Appl Polym Sci 39:749–758
46. Rahman HA (1984) Air permeability on various natural rubber grades. PED Internal Report No. 10. Rubber Research Institute of Malaysia, Kuala Lumpur
47. Hayashi O, Takahashi T, Kurihara H, Ueno H (1981) Monomer unit sequence distribution in partly-epoxidized *trans*-1,4-polyisoprene. Polym J 13:215–223
48. Burfield DR, Gan SN (1975) Non oxidative crosslinking reactions in natural rubber I: determination of crosslinking groups. J Polym Sci Polym Chem Ed 13:2725–2734
49. Davies CKL, Wolfe SV, Gelling IR, Thomas AG (1983) Strain crystallization random copolymers produced by epoxidation of *cis*-1,4-polyisoprene. Polymer 24:107–113
50. Zeng ZQ, Yu HP, Wang QF, Lu G (2008) Effects of coagulation processes on properties of epoxidized natural rubber. J Appl Polym Sci 109:1944–1949
51. Nakason C, Sainamsai W, Kaesaman A, Klinpituksa P, Songklanakarin J (2001) Preparation, thermal and flow properties of epoxidised natural rubber. J Sci Technol 23:415–424
52. Ravanbakhsh M, Khorasani SN, Khalili S (2015) Blending of NR/BR/ENR/EPDM-*g*-GMA by reactive processing for tire sidewall applications: effects of grafting and ENR on curing characteristics, mechanical properties, and dynamic ozone resistance. J Elastomers Plast. doi:10.1177/0095244315580453
53. Gelling IR, Porter M (1990) Chemical modifications of natural rubber. Oxford University Press, Oxford, p 359
54. Saito T, Klinklai W, Kawahara S (2007) Characterization of epoxidized natural rubber by 2D NMR spectroscopy. Polymer 48:750–757
55. Alwaan IM, Hassan A, Piah MAM (2015) Effect of zinc borate on mechanical and dielectric properties of metallocene linear low-density polyethylene/rubbers/magnesium oxide composite for wire and cable applications. Iran Polym J 24:279–288
56. Poh BT, Soo KW (2015) Effect of blend ratio and testing rate on the adhesion properties of pressure-sensitive adhesives prepared from epoxidized natural rubber 25/acrylonitrile–butadiene rubber blend. J Elastomers Plast. doi:10.1177/0095244314568471

57. Johnson T, Thomas S (2000) Effect of epoxidation on the transport behaviour and mechanical properties of natural rubber. Polymer 41:7511–7522
58. Sam ST, Hani N, Ismail H, Noriman N, Ragunathan S (2014) Investigation of epoxidized natural rubber (ENR 50) as a compatibilizer on cogon grass filled low density polyethylene/soya spent flour. Mater Sci Forum 803:310–316
59. Nakason C, Wannavilai V, Kaesaman A (2006) Effect of vulcanization system on properties of thermoplastic vulcanizates based on epoxidized natural rubber/polypropylene blends. Polym Test 25:34–41
60. Margaritis AG, Kalfoglou NK (1987) Miscibility of chlorinated polymers with epoxidized poly(hydrocarbons) 1: epoxidized natural rubber/poly(vinyl chloride) blends. Polymer 28:497–502
61. Rahman MA, Penco M, Peroni I, Ramorino G, Janszen G, Landro LD (2012) Autonomous healing materials based on epoxidized natural rubber and ethylene methacrylic acid ionomers. Smart Mater Struct 21:035014
62. Lin T, Ma S, Lu Y, Guo B (2014) New design of shape memory polymers based on natural rubber crosslinked via Oxa-Michael reaction. ACS Appl Mater Interfaces 6:5695–5703
63. Mahmood WAK, Azarian MH (2015) Thermal, surface, nanomechanical and electrical properties of epoxidized natural rubber (ENR-50)/polyaniline composite films. Curr Appl Phys 15:599–607
64. Abdullah Z, Ibrahim KMYK (2014) Electrical tracking performance of thermoplastic elastomer nanocomposites material under high voltage application. Int J Sci Eng Res 5:708–711
65. Rahman MYA, Ahmad A, Lee TK, Farina Y, Dahlan HM (2012) $LiClO_4$ salt concentration effect on the properties of PVC-modified low molecular weight LENR50-based solid polymer electrolyte. J Appl Polym Sci 124:2227–2233
66. Noor SAM, Ahmad A, Talib IA, Rahman MYA (2011) Effect of ZnO nanoparticles filler concentration on the properties of PEO-ENR50-$LiCF_3SO_3$ solid polymeric electrolyte. Ionics 17:451–456
67. Tan WL, Bakar MA, Bakar NHHA (2013) Effect of anion of lithium salt on the property of lithium salt-epoxidized natural rubber polymer electrolytes. Ionics 19:601–613
68. Mohammad SF, Zainal N, Ibrahim S, Mohamed NS (2013) Conductivity enhancement of (epoxidized natural rubber 50)/poly(ethyl methacrylate)–ionic liquid-ammonium triflate. Int J Electrochem Sci 8:6145–6153
69. Zainal N, Idris R, Sabirin MN (2011) Characterization of (ENR-50)-ionic liquid based electrolyte system. Adv Mater Res 287:424–427
70. Idris R, Glasse MD, Latham RJ, Linford RG, Schlindwein WS (2001) Polymer electrolytes based on modified natural rubber for use in rechargeable lithium batteries. J Power Sour 94:206–211
71. Armand MB (1987) Current state of PEO-based electrolyte. In: MacCallum JR, Vincent CA (eds) Polymer electrolyte reviews, vol 1. Elsevier, London, pp 1–21
72. Rajendran S, Kannan R, Mahendran O (2001) Ionic conductivity studies in poly(methyl methacrylate)-polyethylene oxide hybrid polymer electrolytes with lithium salts. J Power Sour 96:406–410
73. Murata K, Izuchi S, Yoshihisa Y (2000) An overview of the research and development of solid polymer electrolyte batteries. Electrochim Acta 45:1501–1508
74. Polu AR, Kumar R, Rhee HW (2015) Magnesium ion conducting solid polymer blend electrolyte based on biodegradable polymers and application in solid-state batteries. Ionics 21:125–132
75. Armand MB (1986) Polymer electrolytes. Annu Rev Mater Sci 16:245–261
76. Wright PV (1975) Electrical conductivity in ionic complexes of poly(ethylene oxide). Br Polym J 7:319–327
77. Chan CH, Sim LH, Kammer HW, Tan W, Abdul Nasir NH (2011) Ionic transport and glass transition temperature of polyether-salt complexes: dependence on molecular mass of polymer. Mater Res Innov 15:14–17

78. Klongkan S, Pumchusak J (2015) Effects of nano alumina and plasticizers on morphology, ionic conductivity, thermal and mechanical properties of PEO-$LiCF_3SO_3$ solid polymer electrolyte. Electrochim Acta 161:171–176
79. Bushkova OV, Animitsa IE, Lirova BI, Zhukovsky VM (1997) Lithium conducting solid polymer electrolytes based on polyacrylonitrile copolymers: ion solvation and transport properties. Ionics 3:396–404
80. Every HA, Zhou F, Forsyth M, MacFarlane DR (1998) Lithium ion mobility in poly(vinyl alcohol) based polymer electrolytes as determined by ^{7}Li NMR spectroscopy. Electrochim Acta 43:1465–1469
81. Yang JM, Wang SA (2015) Preparation of graphene-based poly(vinyl alcohol)/chitosan nanocomposites membrane for alkaline solid electrolytes membrane. J Membr Sci 477:49–57
82. Ohno H, Matsuda H, Mizoguchi K, Tsuchida E (1982) Demonstration of solid-state cell based on poly(vinylidene fluoride) system containing lithium perchlorate. Polym Bull 7:271–275
83. Ataollahi N, Ahmad A, Lee TK, Abdullah AR, Rahman MYA (2014) Preparation and characterization of PVDF-MG49-$NH_4CF_3SO_3$ based solid polymer electrolyte. E-Polym 14:115–120
84. Le Nest JF, Gandini A, Cheradama H (1988) Crosslinked polyethers as media for ionic conduction. Br Polym J 20:253–268
85. Yusoff SNHM, Sim LH, Chan CH, Hashifudin A, Kammer HW (2013) Solid solution of polymer electrolytes based on modified natural rubber. Polym Res J 7:159–169
86. Klinklai W, Kawahara S, Marwanta E, Mizumo T, Isono Y, Ohno H (2006) Ionic conductivity of highly deproteinized natural rubber having various amount of epoxy group mixed with lithium salt. Solid State Ionics 177:3251–3257
87. Chan CH, Kammer HW, Sim LH, Yusoff SNHM, Hashifudin A, Tan W (2014) Conductivity and dielectric relaxation of Li salt in poly(ethylene oxide) and epoxidized natural rubber polymer electrolytes. Ionics 20:189–199
88. Chan CH, Kammer HW (2015) Polymer electrolytes-relaxation and transport properties. Ionics 21:927–934
89. Gray FM (1991) Solid polymer electrolyte—fundamentals and technological applications. VCH, Weinheim 245
90. Gray FM (1997) Polymer electrolytes. The Royal Society of Chemistry, UK
91. Razali I, Nor WAHWS (2007) Characterization of plasticized and non-plasticised epoxidised natural rubber based polymer electrolyte systems. Solid State Sci Technol 15:147–155
92. Wieczorek W, Siekierski M (1994) A description of the temperature dependence of the conductivity for composite polymeric electrolytes by effective medium theory. J Appl Phys 76:2220–2226
93. Wieczorek W, Zalewska A, Raducha D, Florjanczyk Z, Stevens JR (1998) Composite polyether electrolytes with Lewis acid type additives. J Phys Chem B 102:352–360
94. Wieczorek W, Florjanczyk Z, Stevens JR (1995) Composite polyether based solid electrolytes. Electrochim Acta 40:2251–2258
95. Best AS, Adebahr J, Jacobsson P, MacFarlane DR, Forsyth M (2001) Microscopic interactions in nanocomposite electrolytes. Macromolecules 34:4549–4555
96. Adebahr J, Best AS, Byrne N, Jacobsson P, MacFarlane DR, Forsyth M (2003) Ion transport in polymer electrolytes containing nanoparticulate TiO_2: the influence of polymer morphology. Phys Chem Chem Phys 5:720–725
97. Tan WL, Bakar MA (2014) The effects of magnetite particles and lithium triflate on the thermal behavior and degradation of epoxidized natural rubber (ENR-50). Am-Eurasian J Sustain Agric 8:111–122
98. Chan CH, Kammer HW (2008) Properties of solid solutions of poly(ethylene oxide)/epoxidized natural rubber blends and $LiClO_4$. J Appl Polym Sci 110:424–432

99. Noor SAM, Ahmad A, Rahman MYA, Abu Talib I (2010) Solid polymeric electrolyte of poly(ethylene oxide)-50 % epoxidized natural rubber-lithium triflate (PEO-ENR50-$LiCF_3SO_3$). Nat Sci 2:190–196
100. Noor SAM, Ahmad A, Talib IA, Rahman MYA (2010) Effects of ENR on morphology, chemical interaction and conductivity of PEO-$LiCF_3SO_3$ solid polymer electrolyte. Solid State Sci Technol Lett 18:115–125
101. Aziz M, Chee LC (2005) Preparation and characterization of PVDF/ENR50 polymer blend electrolyte. Solid State Sci Technol 13:126–133
102. Latif F, Aziz M, Katun N, Ali AMM, Yahya MZ (2006) The role and impact of rubber in poly(methyl methacrylate)/lithium triflate electrolyte. J Power Sour 159:1401–1404
103. Ahmad A, Rahman MYA, Ali MLM, Hashim H, Kalam FA (2007) Solid polymeric electrolyte of PVC-ENR-$LiClO_4$. Ionics 13:67–70
104. Mohammad SF, Idris R, Mohamed NS (2010) Conductivity studies of ENR based porton conducting polymer electrolytes. Adv Mater Res 129:561–565
105. Anuar NK, Zainal N, Mohamed NS, Subban RHY (2012) Studies of poly(ethyl methacrylate) complexed with ammonium trifluoromethanesulfonate. Adv Mater Res 501:19–23
106. Chan CH, Kammer HW, Sim LH, Harun MK (2011) Blends of epoxidized natural rubber and thermoplastics. In: Rubber: types, properties and uses. Nova Science Publishers, New York, pp 305–336
107. Sim LH, Gan SN, Chan CH, Kammer HW, Yahya R (2009) Compatibility and conductivity of $LiClO_4$ free and doped polyacrylate-poly(ethylene oxide) blends. Mater Res Innov 13:278–281
108. Mohajir BEE, Heymans N (2001) Changes in structural and mechanical behavior of PVDF with processing and thermomechanical treatments 1: Change in structure. Polymer 42:5661–5667
109. Rahman MYA, Ahmad A, Wahab SA (2009) Electrical properties of a solid polymeric electrolyte of PVC-ZnO-LiClO4. Ionic 15:221–225
110. Noor SAM, Ahmad A, Talib IA, Rahman MYA (2011) Effect of ZnO particles filler concentration on the properties of PEO-ENR50-$LiCF_3SO_3$ solid polymeric electrolyte. Ionics 17:451–456
111. Feuillade G, Perch P (1975) Ion-conductive macromolecular gels and membranes for solid lithium cells. J Appl Electrochem 5:63–69
112. Abraham KM, Alamgir M (1990) Li^+-Conductive solution polymer electrolytes with liquid-like conductivity. J Electrochem Soc 137:1657–1659
113. Mohamed SN, Johari NA, Ali AMM, Harun MK, Yahya MZA (2008) Electrochemical studied on epoxidised natural rubber-based gel polymer electrolytes for lithium-air cells. J Power Sour 183:351–354
114. Latif F, Aziz M, Ali AMM, Yahya MZA (2009) The coagulation impact of 50 % epoxidised natural rubber chain in ethylene carbonate-plasticized solid electrolytes. Macromol Symp 227:62–68
115. Rahman MYA, Ahmad A, Lee TK, Farina Y, Dahlan HM (2011) Effect of ethylene carbonate (EC) plasticizer on poly(vinyl chloride)-liquid 50 % epoxidised natural rubber (LENR50) based polymer electrolyte. Mater Sci Appl 2:818–826
116. Rahman MYA, Ahmad A, Lee TK, Farina Y, Dahlan HM (2012) $LiClO_4$ salt concentration effect on the properties of PVC-modified low molecular weight LENR50-based solid polymer electrolyte. J Appl Polym Sci 124:2227–2233

http://www.springer.com/978-3-319-23662-9

Flexible and Stretchable Electronic Composites

Ponnamma, D.; Sadasivuni, K.K.; Wan, C.; Thomas, S.;
Al-Ali AlMa'adeed, M. (Eds.)

2016, VI, 390 p., Hardcover
ISBN: 978-3-319-23662-9